

Structural and Functional Components of the Skate Sensory Organ Ampullae of Lorenzini

Xing Zhang,^{†,∇} Ke Xia,^{†,∇} Lei Lin,[†] Fuming Zhang,^{‡,Ⓛ} Yanlei Yu,[§] Kalib St. Ange,[†] Xiaorui Han,[†] Eric Edsinger,^{||} Joel Sohn,^{⊥,#} and Robert J. Linhardt^{*,†,‡,§,Ⓛ}

[†]Department of Chemistry and Chemical Biology, Rensselaer Polytechnic Institute, Troy, New York 12180, United States

[‡]Department of Chemical and Biological Engineering, Center for Biotechnology and Interdisciplinary Studies, Rensselaer Polytechnic Institute, Troy, New York 12180, United States

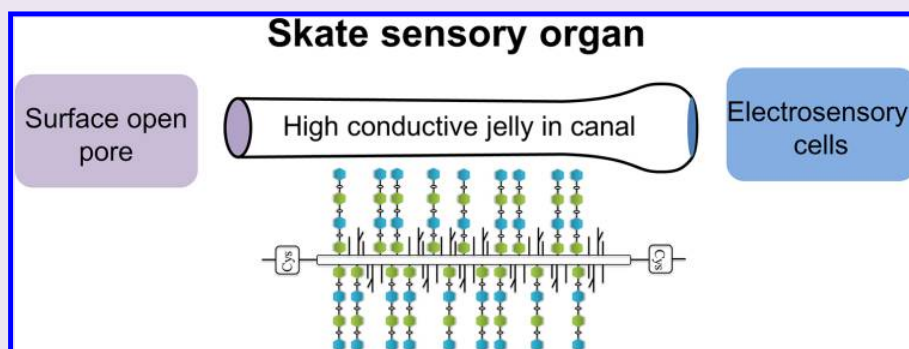
[§]Department of Biology, Center for Biotechnology and Interdisciplinary Studies, Rensselaer Polytechnic Institute, Troy, New York 12180, United States

^{||}Marine Biological Lab, University of Chicago, Chicago, Illinois 60637, United States

[⊥]Department of Electrical Engineering, University of California, Santa Cruz, Santa Cruz, California 95064, United States

[#]Department of Molecular and Cellular Biology, Harvard University, Cambridge, Massachusetts 02138, United States

Supporting Information



ABSTRACT: The skate, a cartilaginous fish related to sharks and rays, possesses a unique electro-sensitive sensory organ known as the ampullae of Lorenzini (AoL). This organ is responsible for the detection of weak electric field changes caused by the muscle contractions of their prey. While keratan sulfate (KS) is believed to be a component of a jelly that fills this sensory organ and has been credited with its high proton conductivity, modern analytical methods have not been applied to its characterization. Surprisingly, total glycosaminoglycan (GAG) analysis demonstrates that the KS from skate jelly is extraordinarily pure, containing no other GAGs. This KS had a molecular weight of 20 to 30 kDa, consisting primarily of *N*-linked KS comprised mostly of a monosulfated disaccharide repeating unit, $\rightarrow 3) \text{Gal} (1 \rightarrow 4) \text{GlcNAc6S} (1 \rightarrow$. Proteomic analysis of AoL jelly suggests that transferrin, keratin, and mucin serve as KS core proteins. Actin and tropomyosin are responsible for assembling the macrostructure of the jelly, and parvalbumin α -like protein and calreticulin regulate calcium and potassium channels involved in the transduction of the electrical signal, once conducted down the AoL by the jelly, serving as the molecular basis for electroreception.

In the late 17th century, an organ of unknown function was discovered by Stefano Lorenzini in a ray¹ and later in the skate and shark. This organ is composed of an external pore open to the seawater environment, canals filled with a gelatinous substance, and at the base of each canal, alveoli. Three-hundred years later, Murray inferred an electro-sensory function,² and Kalminj demonstrated through behavioral experiments that the elasmobranch fishes (rays, skates, and sharks) can detect minute electric fields generated by living organisms and sense earth's geomagnetic fields by use of this organ.³ This organ, in these cartilaginous fish, detects electric field changes caused by the muscle contractions of their prey.⁴

The morphology and neurophysiology of the organ have undergone intensive study;⁵ however, the properties of the jelly like substance that fills the canals are still not well understood. How signals are transduced from an open pore by the jelly to the electro-sensitive cells of the ampullae of Lorenzini (AoL) and to the nervous system remains a subject of debate.^{6,7} The proton conductivity of the jelly contained in the ampullae sensory organ was recently demonstrated to be quite high.⁸

Received: April 10, 2018

Accepted: April 30, 2018

Published: April 30, 2018

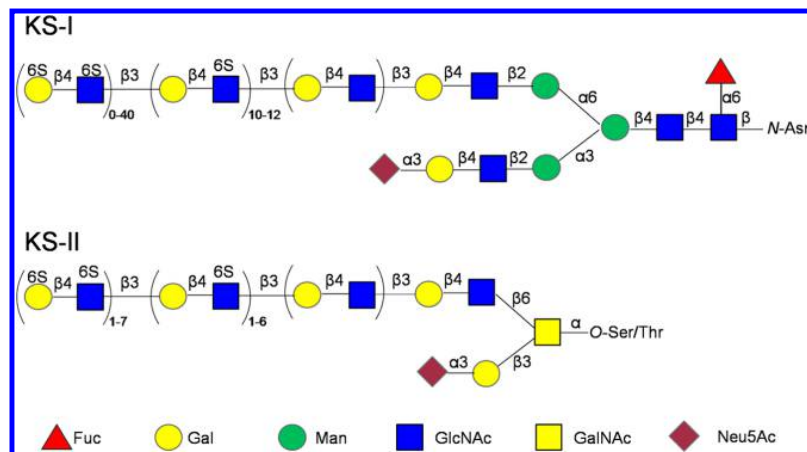


Figure 1. Sulfated poly-*N*-acetylglucosamine chain-linked primarily to either asparagine or serine/threonine residues contained by keratan sulfates. The actual order of the various sulfated and nonsulfated disaccharides occurs somewhat randomly along the chain.

This proton conductivity is only 40-fold lower than that of the best synthetic proton conducting sulfonated fluoropolymer, Nafion, and is higher than any other biological material.^{8,9} Re-examination of the jelly's chemical and physical properties is in order since it was first characterized to be rich in keratan sulfate (KS).¹⁰

KSs are highly sulfated polysaccharides, called glycosaminoglycans (GAGs), which are biosynthesized in the endoplasmic reticulum and Golgi of animals and are covalently attached to a variety of core proteins as a family of proteoglycans (PGs).^{11,12} There are two major types of KS, KS I and II, that differ based on where they are found and their attachment chemistry to core protein^{12,13} (Figure 1). KS I, found primarily in corneal tissue, is an *N*-linked proteoglycan with a chitobiose-trimannosyl linkage region attached to asparagine residues of core proteins including lumican, keratinocan, and mimecan. KS II, found primarily in cartilage, is an *O*-linked proteoglycan attached through an *N*-acetylgalactosamine residue to the serine or threonine residues of core proteins such as aggrecan. KS is just one family of PGs; there are also the heparan sulfate and chondroitin sulfate/dermatan sulfate PG families as well as hyaluronan, a nonsulfated GAG having no core protein.^{14,15} Heparan sulfate, chondroitin sulfate/dermatan sulfate, and hyaluronan are well studied GAGs that are common to all animal cells and which exert important biological roles in development, physiology, and pathophysiology.^{16–18} The biological roles of KS have been less extensively studied and are only beginning to become better understood.^{12,19} Recently, KS has shown importance in inflammation, carcinoma of the female genital tract, macular degeneration, cornea plana type 2 and keratoconus, and neural regeneration and plasticity, suggesting therapeutic applications ranging from regulators of inflammation in arthritis, malignant cellular processes, and suppressors of amyotrophic lateral sclerosis.^{12,19} The *Elasmobranchii*, shark, represents a rich source of cartilage PGs.²⁰ Recent studies have shown that dietary KS from shark cartilage can modulate the gut microbiome.²¹ Moreover, new structurally unique KS molecules, such as a chondroitin sulfate E-KS hybrid GAG from the clam that stimulates neurite outgrowth, are still being discovered.²² Despite these advances, many of the biological and pharmacological roles of KS are still not well understood.

As part of our ongoing structural studies on KS, we previously reported a simplified method for the preparation of corneal KS to examine its growth factor and morphogen binding.²³ We also recently reported that chicken egg white is a rich source for a KS I rich in sialic acid.²⁴ In the current study, we have turned our attention to better understanding the structural and functional roles of the KS and proteins comprising the jelly of the AoL and its role in electroreception.

RESULTS

Recovery of AoL Jelly. Jelly was collected from a commercial catch of big skate (*Raja binoculata*) by pressing the canals of the vertical surface and collected with a mechanical plunger-style pipet at the surface pore. Jelly was collected, stored at 4 °C, and used directly. For long-term storage, an ethanol precipitate of skate jelly was also prepared and the ethanol suspended pellet kept in an explosion-proof freezer at –20 °C until use. The jelly derived components of ethanol precipitate were recovered by removing the ethanol under vacuum. This dried precipitate was insoluble in water or standard buffers but could be dissolved in 8 M urea containing 2 wt % 3-((3-cholamidopropyl) dimethylammonio)-1-propanesulfonate (CHAPS; denaturing buffer). A water insoluble gel could be reformed by removal of urea-CHAPS using a 3000 Da molecular weight cutoff (MWCO) spin column (Figure 2A).

Purification of AoL Jelly Derived GAG and Size Analysis by Polyacrylamide Gel Electrophoresis (PAGE). A portion of the skate AoL jelly ethanol precipitate was first suspended in water and exhaustively treated with actinase E protease to perform GAG analysis. The resulting solution was bound to the strong anion (SAX) exchange membrane of a spin column that was washed to remove protein/peptides, and the GAGs were eluted with 16% NaCl (2.7 M), methanol precipitated, and lyophilized. From 90 mg of skate jelly ethanol precipitate, 6 mg of GAGs was recovered (Figure 2B). The recovered GAG fraction was analyzed by using PAGE with Alcian blue staining. PAGE analysis showed a broad band, expected based on GAG polydispersity, with an average molecular weight of 20 kDa to 30 kDa (Figure S1).

Disaccharide Composition of Skate Jelly Derived GAG by High Performance Liquid Chromatography (HPLC)–Mass Spectrometry (MS) Analysis. Compositional analysis of disaccharides gives important structural information and is a

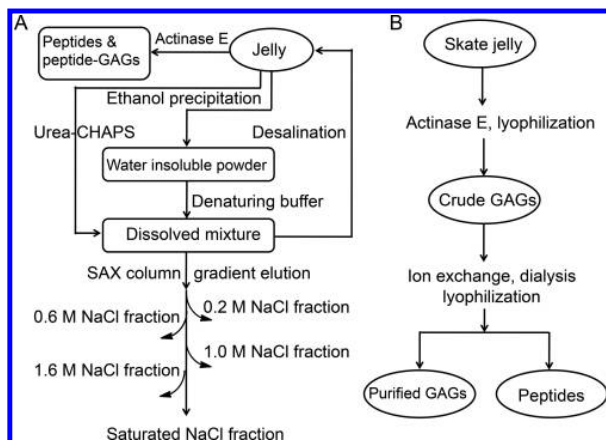


Figure 2. Flowchart of the separation of GAGs, PGs, protein, and peptide components from skate jelly. (A) Purification of skate jelly PGs and proteins. (B) Purification of skate jelly GAGs.

sensitive method for measuring GAG content and variation of GAG structure. Purified GAGs from skate jelly were exhaustively digested with heparin lyase I, II, and III; chondroitin lyase ABC; and keratanase I and II followed by 2-aminoacridone-labeling through reductive amination and analyzed by reversed-phase HPLC-MS. We were surprised to observe no disaccharides from HS, CS, or HA (Figure S2 and Table S1) within the limit of detection (0.1%) of this assay. Only KS disaccharide units were observed, and these corresponded to monosulfated Gal-GlcNAc6S (91.5%) and Gal6S-GlcNAc (8.5%; Gal is galactose, GlcNAc is *N*-acetylglucosamine, and S is sulfo). Both disaccharides have identical mass, corresponding to $C_{14}H_{25}NO_{14}S$, and are only partially resolved by HPLC-MS (Figure S2). Since the *O*-linked shark cartilage KS II generally has a high level of sulfation,²⁵ absence of disulfated monomers suggests that the AoL jelly GAG KS is distinctly different from shark cartilage KS II.

Characterization of KS Structure Using Nuclear Magnetic Resonance (NMR) Spectroscopy.

A combination of one-dimensional (1D) and two-dimensional (2D) NMR was applied to characterize the main structural features and linkage type. The 1D 1H NMR spectrum of the KS sample prepared in the current study was very similar to the KS standard sample from the bovine cornea (Figure 3A), which was previously determined as *N*-linked KS I²³ (Figure 1). The 1D 1H NMR spectrum of KS derived from jelly has a similar crowded region between 3.4 and 4.8 ppm to the corneal KS standard, and the peak observed at 2.02 ppm showed the acetyl groups of the GlcNAc residues (Figure 3A). The minor peaks labeled at 2.98 and 1.69 ppm in the expanded 1D 1H NMR spectrum (Figure 3B), as well as the corresponding cross peaks in the 2D 1H - 1H correlation spectroscopy (COSY) spectrum (Figure 3D), indicated the presence of neuraminic acid. The fucose residue was confirmed by the cross peak of H-6 and C-6 at 1.25/18.3 ppm in the 2D 1H - ^{13}C heteronuclear single quantum coherence (HSQC) spectrum (Figure 3C). It was well-known that Asn is the characteristic residue in the core protein of *N*-linked KS-I, whereas Ser or Thr is always found in *O*-linked KS II.¹³ The minor peak labeled at 2.38 ppm in the expanded 1D 1H NMR spectrum (Figure 3B) combined with the cross peak of H-2/C-2 at 2.38/31.4 ppm in 1H - ^{13}C HSQC spectrum (Figure 3C) strongly indicate the presence of Asn residue, suggesting that the AoL jelly KS had an *N*-linkage, consistent with disaccharide analysis results. By combining 2D COSY, total correlation spectroscopy (TOCSY), and HSQC spectroscopy, the main sugar ring carbon/hydrogen signals could also be assigned (Table S2).

Proteomic Analysis. Proteomic analysis was performed on the ethanol precipitated AoL jelly by dissolving in 6 M guanidinium hydrochloride (GndCl) and dithiothreitol (DTT); then thiol groups were alkylated. The resulting proteins were proteolyzed with trypsin and deglycosylated before their analysis by HPLC-MS. While there is no database for the *R. binoculata* (big skate), several homology databases were used

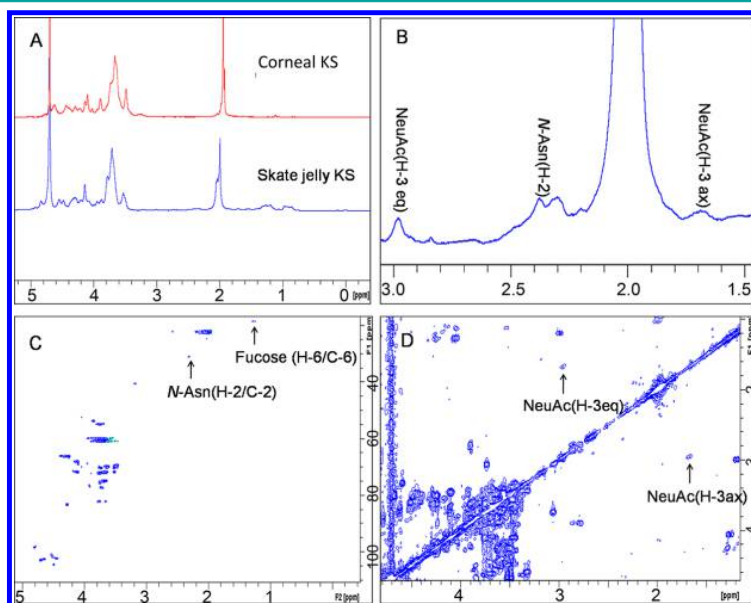


Figure 3. NMR analysis of skate jelly KS. (A) Full 1D 1H NMR spectrum of bovine corneal KS and skate jelly KS. (B) Expanded 1D 1H NMR spectrum (1.5 to 3.0 ppm), (C) 2D HSQC NMR, (D) 2D COSY spectrum of skate jelly KS.

Table 1. Proteins Identified in Proteomic Analysis^a

accession #	protein name	peptides hit	unique peptides (U-Pep)	high- confidence U-pep	coverage %	#AA	MW [Da]
evgc113261_g1_i1-aa	serotransferrin-like	2	2	2	3.83	705	77590
evgc45936_g1_i1-aa	14–3–3 protein epsilon	2	2	2	12.16	255	29024
evgc6235_g1_i1-aa	fucolectin-like	7	2	2	9.55	199	21765
evgc63936_g1_i1-aa	serotransferrin-like (partial)	14	4	3	16.99	259	28697
evgc67709_g1_i1-aa	beta actin	5	4	2	19.05	294	33085
evgc69903_g1_i1-aa	actin, cytoplasmic 1	7	5	4	17.33	375	41650
evgc71152_g1_i1-aa	fructose-1,6-bisphosphatase 1-like	2	2	2	8.53	340	36865
evgc76147_g1_i2-aa	keratin, type II cytoskeletal 8-like	5	4	3	8.11	493	54104
evgc84437_g1_i1-aa	calreticulin	2	2	2	6.71	417	48302
evgc85897_g1_i1-aa	N(G),N(G)-dimethylargininedimethylaminohydrolase 1 isoform X1	12	5	5	25.81	279	29945
evgc86895_g2_i1-aa	g2 tropomyosin alpha-4 chain-like isoform X4	2	2	2	12.8	250	28840
evgc87703_g4_i4-aa	actin, aortic smooth muscle	6	2	2	9.76	328	36355
evgc91154_g7_i1-aa	78 kDa glucose-regulated protein	4	4	4	7.67	652	72207
evgc926_g1_i1-aa	parvalbumin alpha-like	6	5	3	30.22	139	15227
evgc93515_g2_i1-aa	actin, cytoplasmic 1 (partial)	7	2	2	15.53	219	24732
evgc123288_g1_i1-aa	unknown	2	1	1	17.27	110	11707
evgc139999_g1_i1-aa	histone H4	2	2	1	21.36	103	11402
evgc189670_g1_i1-aa	hypothetical protein HELRODRAFT_192394	36	1	1	13.89	144	15873
evgc57113_g1_i1-aa	serotransferrin-like (partial)	7	2	1	13.64	220	23689
evgc74498_g1_i1-aa	beta globin	3	1	1	8.45	142	15724
evgc79213_g1_i1-aa	protein KTI12 homologue	2	2	1	4.04	643	70552
evgc84321_g1_i1-aa	peroxiredoxin-5, mitochondrial	3	1	1	5.82	189	20478
evgc84658_g1_i1-aa	cGMP-dependent 3',5'-cyclic phosphodiesterase isoform X2	44	1	1	2.35	1063	118278
evgc86908_g1_i1-aa	mucin-2-like (partial)	6	2	1	4.08	319	35110
evgc87193_g1_i1-aa	beta-enolase	3	3	1	8.28	435	47272
evgc88139_g4_i1-aa	forkhead-associated domain-containing protein 1	6	1	1	8.93	224	26101
evgc91048_g6_i1-aa	keratin, type I cytoskeletal 19-like	3	1	1	2.72	514	56491
evgc93571_g1_i1-aa	mucosal pentraxin-like	2	1	1	3.1	226	25142
evgc95126_g6_i1-aa	serotransferrin-1-like (partial)	9	2	1	7.11	225	24890

^aThe first 15 proteins listed were identified with two or more, high-confidence unique peptides. Table Note: Accession numbers are from sub-proteome translated from GSE93582_Leucoraja_assembly.fasta. Protein names are from NCBI blast result ([Supporting information Table S3](#)).

(see [Methods](#)) along with the translated transcriptome of *Leucoraja erinacea* (little skate; complete Metazoa (odb9) BUSCOs 88.1%). A search of these databases identified 15 proteins with two or more high confidence unique peptide hits and another 14 proteins with a single high confidence unique peptide hit ([Table 1](#), [Tables S4 and S5](#)). A translated transcriptome of *Leucoraja erinacea* (little skate) gave the highest number of identifications. All identified proteins from homology databases were also found in results searched against the little skate proteome. Several proteins were identified in the AoL jelly that fit current understanding of the structure–function of this sensory organ.⁵ Structural proteins, comprising gels, mucous membranes, and glycocalyx, included actin,^{26,27} serotransferrin-like protein,²⁸ keratin type II cytoskeletal 8-like protein,²⁷ mucin-2,²⁹ and g2 tropomyosin α -4 chain-like isoform X4.^{27,30} With the exception of actin, all of these proteins have NXS/T sequons capable of carrying *N*-linked glycan chains, and indeed, keratin, transferrin, and mucin are known to carry KS GAG chains.^{12,13,31–33} Functional proteins identified in proteomic analysis included parvalbumin α -like; calreticulin can either bind calcium or control calcium channels. Calreticulin is a multifunctional protein that acts as a major

Ca²⁺-binding (storage) protein and mediates the coupling of Ca²⁺ release and influx in a voltage-gated, L-type Ca²⁺ channel,³⁴ the same type of channel identified in little skate AoL.⁵ Parvalbumin α -like, recently identified in the transcriptional analysis, was confirmed in our proteomic analysis and proposed to transduce signals moving from AoL to the nervous system in little skate.⁵

Gelation Properties of KS and Protein Components of AoL Jelly. We next investigated the physical properties of the jelly to understand whether this hydrogel was an ionically and/or covalently cross-linked and to understand the level of structural ordering of AoL jelly. The ethanol precipitated skate jelly could be dissolved in a denaturing solution, consisting of 8 M urea containing 2-wt % CHAPS ([Figure 2B](#)). The dissolved sample when loaded onto a SAX spin column bound and failed to release KS PG when the column was washed with denaturing solution, or even with saturated NaCl (5.4 M) containing 1 M DTT. However, the sample could be completely recovered by washing the SAX spin column with saturated NaCl (5.4 M) in 6 M GndCl containing 50 mM tris(hydroxymethyl)-aminomethane (Tris) and 2.75 mM ethylenediaminetetraacetic acid (EDTA) at pH 6.8. Fractionation of the skate jelly

components was accomplished by first binding the sample dissolved in denaturing solution to the SAX spin column and then eluting by washing with 8 M urea containing 2 wt % CHAPS containing 0.2 M, 0.6 M, 1.0 M, 1.6 M, and saturated NaCl (5.4 M) in 6 M GndCl containing 50 mM Tris and 2.75 mM EDTA at pH 6.8 (Figure 2B). Protein was observed in all fractions, but KS PG was primarily found in the fractions of 0.6 to 1.0 M NaCl urea-CHAPS washes. The proportion of protein and KS GAG in the jelly is approximately equal based on mass determined by protein and GAG assays. Recombining of all of the fractions followed by dialysis failed to reform the gel. Immobilization of GAG KS I onto an SPR chip showed that only the proteins, released from the SAX spin column with 0.2 M NaCl urea-CHAPS, had very weak binding affinity to KS (data not shown), which explains why gel reformation failed, since no significant ionic interaction is present between these protein fractions and carbohydrate.

DISCUSSION

Prior structural studies on AoL jelly GAG relied on monosaccharide analysis, inorganic sulfate determination, and infrared fingerprint identification and provide little detailed information on the fine structure and purity of the GAGs present.^{8,10,35} The first of these studies, a half century ago, suggested that the AoL jelly from skates was comprised of a mixture of proteins and GAGs consisting of sulfated galactose and *N*-acetylglucosamine in equal amounts and small amounts of fucose, consistent, at least in part, with our current understanding of the structure of KS.^{10,35} These studies suggested that these were *O*-linked KS chains based on the presence of serine and threonine in their hydrolyzates, consistent with our understanding of the structures of a cartilage-derived KS II.^{13,33} More recently, Josberger and co-workers showed an infrared spectrum and monosaccharide composition of the major component of AoL jelly from skates, very similar to that published by Doyle, but both studies suggested the presence of multiple types of GAGs (i.e., KS and chondroitin sulfate, suggested by the presence of minor quantities of galactosamine).^{8,10} A paper on the electric organ of the related *Elasmobranchii*, the ray, showed that it contained a chondroitin sulfate/KS PG;³⁶ most KS PGs also contain chondroitin sulfate chains,¹³ and chondroitin sulfate/KS hybrid GAG structures have recently been discovered.²² Thus, we undertook a study of the structure of PG present in the AoL jelly from the skate using the most sophisticated modern analytical methods currently available.

We show that skate jelly PG contains mostly *N*-linked KS I chains of molecular weight 20–30 kDa containing both fucose and sialic acid with structural properties closely resembling bovine corneal KS I (Figure 1). Surprisingly, no other GAGs, i.e., heparan sulfates, chondroitin sulfates, or hyaluronan, are present in the GAG recovered from the jelly. Thus, it is clear that skate jelly cannot contain a typical chondroitin sulfate/KS PG, such as the one found in the electric organ of the ray.³⁶ Moreover, it is very unusual that the only GAG present in skate jelly is KS, as all animal tissues, such as a cornea and cartilage, and all biological fluids examined to date contain multiple types of GAGs. Thus, the AoL jelly from the skate represents the purest source of KS known, and we hypothesize that this might be responsible for its high proton conductivity, allowing the skate and related shark to detect very small fluctuations in electric fields.

KS is a polysaccharide with repeating units bearing electrolyte groups, commonly referred to as a polyelectrolyte.³⁷ Polyelectrolytes are responsible for the stability properties of gels,³⁸ and the dissociation of polyelectrolyte counterions impact the ionic strength and electrical conductivity of such gels.³⁹ Mucin was also identified in AoL jelly in our proteomic analysis. Mucins contain many negatively charged (non-GAG) *O*-linked oligosaccharides⁴⁰ and are rich in galactosamine residues, observed as minor saccharides in previous monosaccharide analyses;^{8,10} moreover, these mucin polyanions might also contribute to the electrical conductivity of AoL jelly.

Skate jelly can be collected, frozen, and freeze-dried, and on rehydration in denaturing buffer, which once removed, permits the reformation of a gel. Biochemical analyses demonstrate that AoL jelly contains both KS I PG and protein components that tightly associate to form a stable, highly structured gel. This is demonstrated by the insolubility of AoL jelly even at high salt concentrations in the absence of a denaturant. Urea-CHAPS is able to solubilize the jelly, which can then be bound to a SAX membrane, but a simple salt wash even in the presence of a DTT reducing agent could not release the bound sample. This suggests that these interactions are more than just ionic interactions or ones only relying on disulfide bonds. A strong ionic denaturant, i.e., GndCl or urea-CHAPS containing salt, is required to recover the sample from a SAX membrane or to fractionate it into protein and KS PG components. But once these individual components of skate jelly are separated, they cannot simply be reconstituted to reform a gel. Moreover, at least one of the isolated protein components was still capable of interacting with KS GAG chains. These biochemical studies suggest the AoL jelly might be a highly organized super structure held together through a combination of protein-carbohydrate (KS GAG chain) interactions, protein-KS core protein interactions, and disulfide covalent cross-linking. Similarly, hydrogels containing both ionic and covalent cross-linking reportedly act as particularly tough viscoelastic adhesives.⁴¹

Proteomic analysis of AoL jelly was undertaken to identify the specific proteins involved in assembling the highly structured AoL hydrogel. Mucin, the major component of mucous gels, and the glycocalyx, known to be a major glycoprotein in mucus along with lactoferrins (serotransferrin-like proteins), were identified in the proteomic analysis. Actin was also found to be a major component of AoL jelly. While actin is most commonly an intracellular structural protein, it can also be found extracellularly and is known to act as a mucin cross-linker in human airway mucus,²⁶ as well as a structural protein in the skin mucus of farmed gilthead seabream (*Sparus aurata*).²⁷ Tropomyosin, a protein that wraps around actin filaments contributing to its superstructure,³⁰ was also identified in AoL jelly. Proteomic analysis identified three potential KS-core proteins, mucin, known to contain either *N*- or *O*-linked KS GAG chains along with multiple anionic *O*-linked oligosaccharides,^{13,40} and serotransferrin, with *N*-linked KS.³² One protein identified in proteomic analysis, keratin, not only can bind to the KS GAG chain⁴² but is also reported to be glycosylated with KS.³¹ Keratin is also a structural protein in the skin mucus of farmed gilthead seabream.²⁷ Mass spectrometry results from the two keratins identified in the skate have unique peptides that differ from any proteins in the NCBI *Homo sapiens* proteome (Table S6). Therefore, we can rule out that these peptides result from human contamination. On the basis of our glycan analysis results, we conclude that the

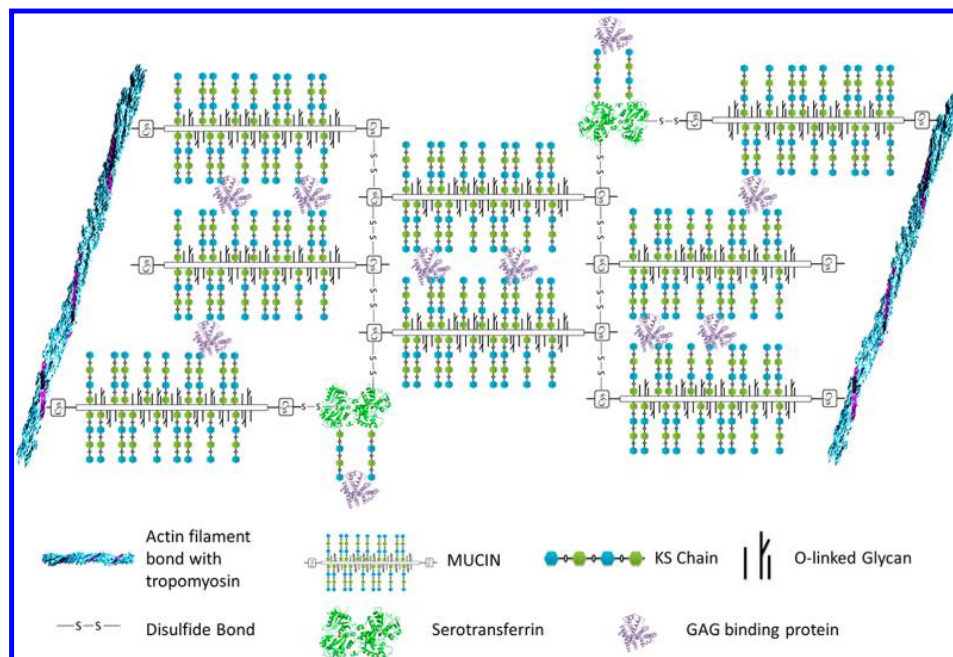


Figure 4. Proposed structure of gel comprising Lorinzini jelly.

structure of AoL jelly is comprised of highly pure KS in the absence of any other GAGs. While AoL jelly KS resembles the KS in the cornea, another sensory organ tissue rich in *N*-linked KS I.¹³ In our postulated model of AoL jelly is a hydrogel held together in three ways, through noncovalent protein–protein interactions, covalent disulfide bonds, and ionic protein–GAG interactions (Figure 4). The KS PG mucin is held together by actin and tropomyosin that bind to the mucin core protein through protein–protein interactions. Moreover, it is well-known that mucin is also cross-linked through terminal disulfide bonds,⁴³ which may also stabilize AoL jelly. Keratin type II cytoskeletal-like protein is capable of ionically binding to the KS GAG chains of either mucin or serotransferrin KS-PGs, but our studies suggest that this protein–carbohydrate interaction is insufficient for gelation.

Serotransferrin belongs to the lactoferrin family, which reportedly has antibacterial,⁴⁴ antifungal,⁴⁵ and antiviral activities.⁴⁶ Since the AoL of the skate has an open pore to seawater, containing a complex collection of microorganisms, we speculate that serotransferrin might also play an anti-infective role in addition to serving a structural role as a KS-PG.

We hypothesize that the major functional property of AoL jelly, high proton conductivity, makes use of a highly structurally organized polyelectrolyte, KS (Figure 5). This sulfated polysaccharide, capable of conductivities comparable to synthetic polymers such as Nafion used in fuel cells,⁸ is used to conduct weak electrical signals from the external pore down the

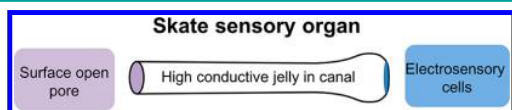


Figure 5. Function of AoL: to serve as a highly structured polyelectrolyte to propagate weak electrical signals from the outside pore exposed to seawater to the nerve fibers of the skate CNS.

low-resistance gel-filled channel of the AoL. This weak electrical signal is then transduced across a membrane through a $\text{Ca}^{2+}/\text{K}^{+}$ channel to nerve fibers leading to the skate's central nervous system (CNS). KS could associate with Ca^{2+} counterions which may act as a calcium reserve.^{47,48} Proteomic analysis also identified ancillary proteins in AoL jelly, including parvalbumin α -like protein and calreticulin that regulate calcium and potassium channels and serve as the molecular basis for electroreception.^{5,34} Proteomic and biochemical analyses suggest that high proton conductivity coupled with control of cation movement are critically important in the functioning of these sensory organs.

The structural model provided in Figure 4 represents only one possible model that is consistent with the structural components present and the functional properties of the AoL (Figure 5). This model will need to be revised as more structural and functional information becomes available, including a better understanding of the cationic components within skate jelly. The presence of cations within skate jelly is very difficult to assess because of the uncontrolled presence of cation-rich seawater during the collection of such samples.

METHODS

Materials. AoL jelly was obtained from visible surface pores on the skin of big skates and preserved both as a sample of jelly stored at 4 °C and as an ethanol precipitate.⁸ Bovine corneal KS standard was primarily produced in our laboratory as described previously.²³ Actinase E was obtained from Kaken Biochemicals (Japan). Recombinant *Flavobacterium* heparin lyases I, II, and III, and chondroitin lyase ABC from *Proteus vulgaris* were expressed using *Escherichia coli* strains. Keratanase I was obtained from Seikagaku (Japan). Keratanase II from *Bacillus* sp. was developed and expressed using *Escherichia coli* strains. The 2-aminoacridone, urea, and CHAPS were purchased from Sigma (St. Louis, MO, USA). All other used chemicals were of analytical grade. Unsaturated disaccharide standards of CS ($0\text{S}_{\text{CS-0}}$: $\Delta\text{UA-GalNAc}$; $4\text{S}_{\text{CS-A}}$: $\Delta\text{UA-GalNAc4S}$; $6\text{S}_{\text{CS-C}}$: $\Delta\text{UA-GalNAc6S}$; 2S_{CS} : $\Delta\text{UA2S-GalNAc}$; $2\text{S}4\text{S}_{\text{CS-B}}$: $\Delta\text{UA2S-GalNAc4S}$; $2\text{S}6\text{S}_{\text{CS-D}}$: $\Delta\text{UA2S-GalNAc6S}$; $4\text{S}6\text{S}_{\text{CS-E}}$: $\Delta\text{UA-GalNAc4S6S}$; TriS_{CS} :

Δ UA2S-GalNAc4S6S), unsaturated disaccharide standards of HS ($0S_{HS}$: Δ UA-GlcNAc; NS_{HS} : Δ UA-GlcNS; $6S_{HS}$: Δ UA-GlcNAc6S; $2S_{HS}$: Δ UA2S-GlcNAc; $2SNS_{HS}$: Δ UA2S-GlcNS; $NS6S_{HS}$: Δ UA-GlcNS6S; $2S6S_{HS}$: Δ UA2S-GlcNAc6S; $TriS_{HS}$: Δ UA2S-GlcNS6S), and an unsaturated disaccharide standard of HA ($0S_{HA}$: Δ UA-GlcNAc), where Δ UA is 4-deoxy- α -L-threo-hex-4-enopyranosyluronic acid, were purchased from Iduron (UK).

Purification of GAGs from Skate Jelly. A 90 mg sample of freeze-dried skate jelly was suspended in 9 mL of water, proteolyzed at 55 °C with 10 mg mL⁻¹ actinase E for 24 h, and freeze-dried. The resulting sample was dissolved in 5 mL of a solution of denaturing buffer (8 M urea containing 2 wt % CHAPS), bound to a Vivapure Q Maxi H spin column, washed twice with 10 mL of denaturing buffer, and washed three-times with 10 mL of 0.2 M NaCl. The GAG components were then eluted from the spin column with three 10 mL volumes of 16% NaCl, and the salt of these fractions was removed by dialysis (MWCO 500–1000 Da) against distilled water and freeze-dried to recover the purified GAGs.

Size Analysis by PAGE. PAGE was used to determine the molecular weight properties of GAGs. The purified GAGs were separated by a 15% total acrylamide (15% T) containing 14.08% (w/v) acrylamide, 0.92% (w/v) *N,N'*-methylene-bis-acrylamide, and 5% (w/v) sucrose. All monomer solutions were prepared in resolving buffer (0.1 M boric acid, 0.1 M Tris, 0.01 M disodium EDTA, pH 8.3). Stacking gel monomer solution was prepared in resolving buffer, containing 4.75% (w/v) acrylamide and 0.25% (w/v) *N,N'*-methylene-bis-acrylamide and the pH adjusted to 6.3 using HCl. A 10 cm \times 7 mm diameter resolving gel column was cast from 4 mL of 15% resolving gel solution containing 4 μ L of tetramethylethylenediamine and 12 μ L of 10% ammonium persulfate. A stacking gel was cast from 1 mL of stacking gel monomer solution containing 1 μ L of tetramethylethylenediamine and 30 μ L of 10% ammonium persulfate. Phenol red dye was added to the sample for visualization of the ion front during electrophoresis. In each lane, \sim 5 μ g of sample was subjected to electrophoresis. A standard composed of a mixture of heparin oligosaccharides with known molecular weights was prepared enzymatically from bovine lung heparin.⁴⁹ The gel was visualized with alcian blue staining and then digitized with UN-Scan-it, and molecular weight was calculated.⁴⁹

Disaccharide Analysis. Purified GAGs (10 μ g) was dissolved in 300 μ L of digestion buffer (50 mM ammonium acetate, 2 mM calcium chloride). Recombinant heparin lyase I, II, and III; chondroitin lyase ABC; and keratanase I and II (10 mU of each enzyme) were then added to the reaction buffer and placed in a 37 °C incubator, overnight. Removing the enzymes by passing through a 3000 Da MWCO spin column terminated the reaction. The filter unit was washed twice with 200 μ L of distilled water, and the combined fractions were finally lyophilized. The dried samples were 2-aminoacridone-labeled by adding 10 μ L of 0.1 M 2-aminoacridone in dimethyl sulfoxide/acetic acid (17/3, v/v) incubating at RT for 10 min, followed by adding 10 μ L of 1 M aqueous NaBH₃CN and incubating for 1 h at 45 °C. The resulting samples were centrifuged at 13 200 rpm for 10 min. Finally, each supernatant was collected and stored in a light resistant container at RT until analyzed via HPLC-MS on an Agilent 1200 LC/MSD instrument (Agilent Technologies, Inc. Wilmington, DE) equipped with a 6300 ion-trap and a binary pump. The column used was a Poroshell 120 C18 column (3.0 \times 50 mm, 2.7 μ m, Agilent, USA) at 45 °C. Eluent A was 50 mM ammonium acetate solution, and eluent B was methanol. The mobile phase passed through the column at a flow rate of 250 μ L/min with 10 min linear gradients of 10–35% solution B. The electrospray interface was set in negative ionization mode with a skimmer potential of -40.0 V, a capillary exit of -40.0 V, and a source temperature of 350 °C, to obtain the maximum abundance of the ions in a full-scan spectrum (300–850 Da). Nitrogen (8 L/min, 40 psi) was used as a drying and nebulizing gas.

Structural Analysis by NMR. The NMR spectra of the skate jelly KS and bovine corneal KS standard were obtained on a Bruker 600 MHz (14.1 T) standard-bore NMR spectrometer equipped with a ¹H/²H/¹³C/¹⁵N cryoprobe with z-axis gradients. Jelly KS (5 mg) or

bovine corneal KS (5 mg) was dissolved in 0.4 mL of 99.6% D₂O centrifuged at 5000g for 2 min and lyophilized. The process was repeated twice, and the final sample was dissolved in 0.4 mL of 99.96% D₂O. ¹H spectroscopy, ¹³C spectroscopy, ¹H–¹H correlated spectroscopy (COSY), ¹H–¹³C heteronuclear single quantum coherence spectroscopy (HSQC), and ¹H–¹H total correlation spectroscopy (TOCSY) experiments were all carried out at 298 K.

PAGE and BCA Assay of Keratan Sulfate-Proteoglycan Fractions. Skate jelly dissolved in urea-CHAPS can be fractionated using SAX spin columns eluted in a stepwise fashion with gradient concentrations of sodium chloride in denaturing buffer (8 M urea containing 2 wt % CHAPS). The skate jelly crude was dissolved in a 5 mL denaturing buffer and bound to a Vivapure Q Maxi H spin column, which had been pre-equilibrated with denaturing buffer. Different keratan sulfate-proteoglycan components were eluted by washing with three 10 mL volumes of 0.2, 0.6, 1.0, and 1.6 M and saturated (5.4 M) aqueous sodium chloride. The salt of each fraction was removed with a 3000 Da MWCO spin column, and the resulting freeze-dried products were quantified by Pierce bicinchoninic acid (BCA) protein assay.

Proteoglycans Interaction Studies. The sensor CMS chip was from GE healthcare (Uppsala, Sweden). SPR measurements were performed on a BIAcore 3000 (GE healthcare, Uppsala, Sweden) operated using BIAcore 3000 control and BIAevaluation software (version 4.0.1). KS and two protein components, eluted by 0.6 M and saturated (5.4 M) aqueous NaCl, respectively, were immobilized on research grade CMS chips using ethyl(dimethylaminopropyl)-carbodiimide/*N*-hydroxysuccinimide according to the standard amine coupling protocol. KS or protein samples were then diluted in HBS-EP buffer (0.01 M HEPES, 0.15 M NaCl, 3 mM EDTA, 0.005% surfactant P20, pH 7.4) and injected at a flow rate of 50 μ L/min with HBS-EP buffer as a running buffer to measure the molecular interactions between KS/protein or protein–protein. At the end of the sample injection, HBS-EP buffer was flowed over the sensor surface to facilitate dissociation. The sensor surface was fully regenerated by injecting with 50 μ L of 2 M NaCl. The response was monitored as a function of time (sensorgram) at 25 °C.

Sample Process for Proteomic Study. The sample was dissolved in 6 M GndCl and 50 mM DTT for 1 h, incubated in the dark with 150 mM iodoacetamide for 30 min, and buffer exchanged three times to remove GndCl (to <50 mM). The sample was digested with Trypsin Gold (Promega, Madison, WI) with its standard in-solution digestion protocol. After digestion, the trypsin was deactivated by boiling for 5 min. PNGase F (Sigma-Aldrich St. Louis, MO) was next used to remove N-glycan by a standard protocol. PNGase F and Trypsin were removed using a 10K molecular cutoff concentration spin column (Millipore, St. Louis, MO). The peptide mixture in the flow-through was recovered and used in proteomic analysis.

Nano HPLC MS/MS. The resulting peptide mixtures were analyzed using an Agilent 1200-Series LC system coupled to an LTQ-Orbitrap mass spectrometer (Thermo Fisher Scientific, Waltham, MA USA). The LC system was equipped with a 75 μ m ID, 15 μ m tip, 105 mm picochip ((New Objective, Cambridge, MA) bed packed with 5 μ m BioBasic (Thermo Fisher Scientific, Waltham, MA USA) C18 and 300A resin. Sample loading was finished in 2% buffer B (98% acetonitrile in 0.1% formic acid) in 10 min. Elution was achieved with a gradient of 15–90% B in total 90 min. The flow rate was passively split from 0.3 mL/min to 200 nL/min. The mass spectrometer was operated in data-dependent mode to switch between MS and MS/MS. The five most intense ions were selected for fragmentation in the linear ion trap using collision-induced dissociation.

Subproteome Databases Building. There is no subproteome available for *R. binoculata* (big skate), and the proteome of the *Chondrichthyes* class is not systematically finished. While *R. binoculata* belongs to the *Rajidae* family, *Elasmobranchii* subclass, and *Chondrichthyes* class, several homology databases were selected for testing, including TrEMBL *Rajidae*, TrEMBL *Elasmobranchii*, and TrEMBL *Chondrichthyes*. TrEMBL/Swiss-Prot zebrafish (*Danio rerio*) was also used to increase the possibility of hits.

Another strategy translated a very closely related transcriptome into a subproteome. *Leucoraja erinacea* (little skate) is in the same *Rajidae* family and was selected. Little skate does not have a subproteome but it has a relatively complete transcriptome. This NCBI GEO skate transcriptome (accession GSE93582 and transcriptome file GSE93582_Leucoraja_assembly.fasta) was run through EvidentialGene⁵⁰ to provide transcript quality filtering of the transcriptome, and then evaluated using BUSCO. A BLAST database was built, and the transcriptome was annotated using InterProScan5 and by reciprocal best hit to human and zebrafish.

MS/MS Results Searching. MS/MS results were searched against each subproteome database mentioned above. The SEQUEST search algorithm was used from Proteome Discoverer (Thermo Fisher Scientific, Waltham, MA USA). Enzyme specificity was set for trypsin with a maximum of three missed cleavages allowed. Carbamidomethylation of cysteine and oxidation of methionine were included as variable modifications. For most tests, the mass error of parent ions was set to 6 ppm instead of 10 ppm for better accuracy and 0.8 Da for fragment ions.

Protein Identification Summary. Commonly accepted criteria for high-confidence peptide identifications were used (xCorr 1.8 for +1, 2.5 for +2, 3.5 for +3) to screen peptides.⁵¹ Proteins containing two or more high-confidence unique peptides were included in the table and are considered high-confidence protein ID results with low false positive rates of protein identification. Proteins containing only one high-confidence unique peptide are also listed in the table for reference. Their number of high-confidence unique peptides discovered was possibly limited due to several reasons. Since some proteins translated from *Leucoraja erinacea* (little skate) transcriptome are fragments instead of the whole sequence, the protein sequence shows some differences between *R. binoculata* (big skate) and *Leucoraja erinacea* (little skate), as well as the incomplete subproteome available for *R. binoculata* (big skate).

■ ASSOCIATED CONTENT

Supporting Information

The Supporting Information is available free of charge on the ACS Publications website at DOI: 10.1021/acscchembio.8b00335.

Detailed Experimental materials and methods, additional figures, tables, and spectral data (PDF)

■ AUTHOR INFORMATION

Corresponding Author

*E-mail: linhar@rpi.edu.

ORCID

Fuming Zhang: 0000-0003-2803-3704

Robert J. Linhardt: 0000-0003-2219-5833

Author Contributions

^vX.Z. and K.X. are equal contributors. X.Z. and K.S.A. performed the NMR studies and characterization of KS. L.L., X.Z., and Y.Y. performed the fractionation and gelation studies. X.H. and K.X. performed the MS and proteomics studies. E.E. performed little skate transcriptome analyses. J.S. collected the jelly samples. J.S., K.X., and R.J.L. designed the study and wrote the manuscript.

Notes

The authors declare no competing financial interest.

■ ACKNOWLEDGMENTS

This work was supported by National Institutes of Health grants HL62244 and HL125371 to R.J.L. and Vetlesen Foundation funding of E.E.'s Research Fellow position. E.E. wishes to thank D. Gilbert for guidance on the use of

EvidentialGene and general strategies in *de novo* transcriptome assembly.

■ REFERENCES

- (1) Lorenzini, S. (1678) *Osservazioni Intorno Alle Torpedini*, Per L'Onofri, Firenze.
- (2) Murray, R. W. (1962) The response of the ampullae of Lorenzini of elasmobranchs to electrical stimulation. *J. Exp. Biol.* 39, 119–128.
- (3) Kalmijn, A. J. (1982) Electric and magnetic field detection in elasmobranch fishes. *Science* 218, 916–918.
- (4) Camperi, M., Tricas, T. C., and Brown, B. R. (2007) From morphology to neural information: The electric sense of the skate. *PLoS Comput. Biol.* 3, e113.
- (5) Bellono, N. W., Leitch, D. B., and Julius, D. (2017) Molecular basis of ancestral vertebrate electroreception. *Nature* 543, 391–396.
- (6) Brown, B. R. (2003) Neurophysiology: Sensing temperature without ion channels. *Nature* 421, 495.
- (7) Fields, R. D. (2007) The shark's electric sense. *Sci. Am.* 297, 74–81.
- (8) Josberger, E. E., Hassanzadeh, P., Deng, Y., Sohn, J., Rego, M. J., Amemiya, C. T., and Rolandi, M. (2016) Proton conductivity in ampullae of Lorenzini jelly. *Sci. Adv.* 2, e1600112.
- (9) Sone, Y., Ekdunge, P., and Simonsson, D. (1996) Proton conductivity of Nafion 117 as measured by a four-electrode AC impedance method. *J. Electrochem. Soc.* 143, 1254–1259.
- (10) Doyle, J. (1967) The 'Lorenzan sulphates'. A new group of vertebrate mucopolysaccharides. *Biochem. J.* 103, 325–330.
- (11) Funderburgh, J. L. (2002) Keratan sulfate biosynthesis. *IUBMB Life* 54, 187–194.
- (12) Caterson, B., and Melrose, J. (2018) Keratan sulphate, a complex glycosaminoglycan with unique functional capability. *Glycobiology* 28, 182–206.
- (13) Funderburgh, J. L. (2000) Keratan sulfate: Structure, biosynthesis and function. *Glycobiology* 10, 951–958.
- (14) Esko, J. D., Kimata, K., and Lindahl, U. Proteoglycans and sulfated glycosaminoglycans. In *Essentials of Glycobiology*, 2nd ed., (Varki, A., Cummings, R. D., Esko, J. D., Freeze, H. H., Stanley, P., Bertozzi, C. R., Hart, G. W., and Etzler, M. E., Eds.) Cold Spring Harbor Laboratory Press, New York, 2009, Chapter 16.
- (15) Couchman, J. R., and Pataki, C. A. (2012) An introduction to proteoglycans and their localization. *J. Histochem. Cytochem.* 60, 885–897.
- (16) Kamhi, E., Joo, E. J., Dordick, J. S., and Linhardt, R. J. (2013) Glycosaminoglycans in infectious disease. *Biol. Rev. Camb. Philos. Soc.* 88, 928–943.
- (17) Belting, M. (2014) Glycosaminoglycans in cancer treatment. *Thromb. Res.* 133, S95–S101.
- (18) Mikami, T., and Kitagawa, H. (2017) Sulfated glycosaminoglycans: their distinct roles in stem cell biology. *Glycoconjugate J.* 34, 725–735.
- (19) Pomin, V. H. (2015) Keratan sulfate: An up-to-date review. *Int. J. Biol. Macromol.* 72, 282–289.
- (20) Higashi, K., Takeuchi, Y., Mukuno, A., Tomitori, H., Miya, M., Linhardt, R. J., and Toida, T. (2015) Composition of glycosaminoglycans in *Elasmobranchs* including several deep-sea sharks: Identification of chondroitin/dermatan sulfate from the dried fins of *Isurus oxyrinchus* and *Prionace glauca*. *PLoS One* 10, e0120860.
- (21) Shang, Q., Li, Q., Zhang, M., Song, G., Shi, J., Jiang, H., Cai, C., Hao, J., Li, G., and Yu, G. (2016) Dietary keratan sulfate from shark cartilage modulates gut microbiota and increases the abundance of *Lactobacillus* spp. *Mar. Drugs* 14, 224.
- (22) Higashi, K., Takeda, K., Mukuno, A., Okamoto, Y., Masuko, S., Linhardt, R. J., and Toida, T. (2016) Identification of keratan sulfate disaccharide at C-3 position of glucuronate of chondroitin sulfate from *Macra chinensis*. *Biochem. J.* 473, 4145–4158.
- (23) Weyers, A., Yang, B., Solakylidirim, K., Yee, V., Li, L., Zhang, F., and Linhardt, R. J. (2013) Isolation of bovine corneal keratan sulfate and its growth factor and morphogen binding. *FEBS J.* 280, 2285–2293.

- (24) Fu, L., Sun, X., He, W., Cai, C., Onishi, A., Zhang, F., Linhardt, R. J., and Liu, Z. (2016) Keratan sulfate glycosaminoglycan from chicken egg white. *Glycobiology* 26, 693–700.
- (25) Zhang, Y., Kariya, Y., Conrad, A. H., Tasheva, E. S., and Conrad, G. W. (2005) Analysis of keratan sulfate oligosaccharides by electrospray ionization tandem mass spectrometry. *Anal. Chem.* 77, 902–910.
- (26) Leigh, M. W. (2002) Airway secretions. In *Basic Mechanisms of Pediatric Respiratory Disease* (Haddad, G. G., Abman, S. H., and Chernick-Mellins, V., Eds.) PMPH-USA, Chapter 35.
- (27) Jurado, J., Fuentes-Almagro, C. A., Guardiola, F. A., Cuesta, A., Esteban, M.Á., and Prieto-Álamo, M. J. (2015) Proteomic profile of the skin mucus of farmed gilthead seabream (*Sparus aurata*). *J. Proteomics* 120, 21–34.
- (28) Singh, P. K., Parsek, M. R., Greenberg, E. P., and Welsh, M. J. (2002) A component of innate immunity prevents bacterial biofilm development. *Nature* 417, 552–555.
- (29) Thornton, D. J., Rousseau, K., and McGuckin, M. A. (2008) Structure and function of the polymeric mucins in airways mucus. *Annu. Rev. Physiol.* 70, 459–486.
- (30) von der Ecken, J., Müller, M., Lehman, W., Manstein, D. J., Penczek, P. A., and Raunser, S. (2015) Structure of the F-actin-tropomyosin complex. *Nature* 519, 114–117.
- (31) Schafer, I. A., and Sorrell, J. M. (1993) Human keratinocytes contain keratin filaments that are glycosylated with keratan sulfate. *Exp. Cell Res.* 207, 213–219.
- (32) Magro, G., Perissinotto, D., Schiappacassi, M., Goletz, S., Otto, A., Müller, E. C., Bisceglia, M., Brown, G., Ellis, T., Grasso, S., Colombatti, A., and Perris, R. (2003) Proteomic and postproteomic characterization of keratan sulfate-glycanated isoforms of thyroglobulin and transferrin uniquely elaborated by papillary thyroid carcinomas. *Am. J. Pathol.* 163, 183–96.
- (33) Hang, H. C., and Bertozzi, C. R. (2005) The chemistry and biology of mucin-type O-linked glycosylation. *Bioorg. Med. Chem.* 13, 5021–5034.
- (34) Kwon, M. S., Park, C. S., Choi, K., Ahn, J., Kim, J. I., Eom, S. H., Kaufman, S. J., Song, W. K., and Park, C.-S. (2000) Calreticulin couples calcium release and calcium influx in integrin-mediated calcium signaling. *Mol. Biol. Cell* 11, 1433–1443.
- (35) How, M. J., Jones, J. V. S., and Doyle, J. (1969) Comparative studies of Lorinzini jelly from two species of elasmobranch: Part I. Preparation of glycopeptides. *Carbohydr. Res.* 11, 207–216.
- (36) Carlson, S. S., Iwata, M., and Wight, T. N. (1996) A chondroitin sulfate/keratan sulfate proteoglycan, PG-1000, forms complexes which are concentrated in the reticular laminae of electric organ basement membranes. *Matrix Biol.* 15, 281–292.
- (37) Seyrek, E., and Dubin, P. (2010) Glycosaminoglycans as polyelectrolytes. *Adv. Colloid Interface Sci.* 158, 119–129.
- (38) Monteux, C., Williams, C. E., Meunier, J., Anthony, O., and Bergeron, V. (2004) Adsorption of oppositely charged polyelectrolyte/surfactant complexes at the air/water interface: Formation of interfacial gels. *Langmuir* 20, 57–63.
- (39) Rumyantsev, A. M., Pan, A., Roy, S. G., De, P., and Kramarenko, E. Y. (2016) Polyelectrolyte gel swelling and conductivity vs counterion type, cross-linking density, and solvent polarity. *Macromolecules* 49, 6630–6643.
- (40) Brockhausen, I., and Stanley, P. (2015) O-GalNAc Glycans, In *Essentials of Glycobiology*, 3rd ed. (Varki, A., Cummings, R. D., Esko, J. D., Stanley, P., Hart, G. W., Aebi, M., Darvill, A. G., Kinoshita, T., Packer, N. H., Prestegard, J. H., Schnaar, R. L., Peter, H., and Seeberger, P. H., Eds.), Cold Spring Harbor Laboratory Press, Cold Spring Harbor, NY, Chapter 10.
- (41) Li, J., Celiz, A. D., Yang, J., Yang, Q., Wamala, I., Whyte, W., Seo, B. R., Vasilyev, N. V., Suo, Z., Mooney, D. J., and Vlassak, J. J. (2017) Tough adhesives for diverse wet surfaces. *Science* 357, 378–381.
- (42) Roth, M., Papakonstantinou, E., and Karakiulakis, G. (2011) Biological function of glycosaminoglycan, In *Carbohydrate Chemistry, Biology and Medical Applications*, 1st ed. (Garg, H. G., Cowman, M. K., and Hales, C., Eds.), Elsevier Science, Chapter 9.
- (43) Perez-Vilar, J., Eckhardt, A. E., DeLuca, A., and Hill, R. L. (1998) Porcine, submaxillary mucin forms disulfide-linked multimers through its amino-terminal D-domains. *J. Biol. Chem.* 273, 14442–14449.
- (44) Farnaud, S., and Evans, R. W. (2003) Lactoferrin—a multifunctional protein with antimicrobial properties. *Mol. Immunol.* 40, 395–405.
- (45) Viejo-Díaz, M., Andrés, M. T., and Fierro, J. F. (2004) Modulation of *in vitro* fungicidal activity of human lactoferrin against *Candida albicans* by extracellular cation concentration and target cell metabolic activity. *Antimicrob. Agents Chemother.* 48, 1242–1248.
- (46) van der Strate, B. W., Beljaars, L., Molema, G., Harmsen, M. C., and Meijer, D. K. (2001) Antiviral activities of lactoferrin. *Antiviral Res.* 52, 225–239.
- (47) Du, J., Hincke, M. T., Rose-Martel, M., Hennequet-Antier, C., Brionne, A., Cogburn, L. A., Nys, Y., and Gautron, J. (2015) Identifying specific proteins involved in eggshell membrane formation using gene expression analysis and bioinformatics. *BMC Genomics* 16, 792.
- (48) Ha, Y. W., Son, M. J., Yun, K. S., and Kim, Y. S. (2007) Relationship between eggshell strength and keratan sulfate of eggshell membranes. *Comp. Biochem. Physiol., Part A: Mol. Integr. Physiol.* 147, 1109–1115.
- (49) Edens, R. E., Al-Hakim, A., Weiler, J. M., Rethwisch, D. G., Fareed, J., and Linhardt, R. J. (1992) Gradient polyacrylamide gel electrophoresis for determination of the molecular weights of heparin preparations and low-molecular-weight heparin derivatives. *J. Pharm. Sci.* 81, 823–827.
- (50) Gilbert, D. Gene-omes built from mRNA seq not genome DNA. Presented at 7th Annual Arthropod Genomics Symposium, Notre Dame, IN, 2013, DOI: 10.7490/fl1000research.1112594.1.
- (51) Kang, R., Wan, J., Arstikaitis, P., Takahashi, H., Huang, K., Bailey, A. O., Thompson, J. X., Roth, A. F., Drisdell, R. C., Mastro, R., Green, W. N., Yates, J. R., III, Davis, N. G., and El-Husseini, A. (2008) Neural palmitoyl-proteomics reveals dynamic synaptic palmitoylation. *Nature* 456, 904–909.